Chapter

Rigorous Analysis of the Propagation in Metallic Circular Waveguide with Discontinuities Filled with Anisotropic Metamaterial

Hedi Sakli and Wyssem Fathallah

Abstract

In this chapter, we present an extension of the rigorous analysis of the propagation of electromagnetic waves in magnetic transverse (TM) and transverse electric (TE) modes in a metallic circular waveguide partially filled with anisotropic metamaterial. In our analysis, the design of waveguide filters with uniaxial discontinuities is based on the determination of the higher-order modes, which have been analyzed and exploited. Below the cutoff frequency, the back backward waves can propagate in an anisotropic material. The numerical results with our MATLAB code for TM and TE modes were compared to theoretical predictions. Good agreements have been obtained. We analyzed a waveguide filters filled with partially anisotropic metamaterial using the mode matching (MM) technique based on the Scattering Matrix Approach (SMA), which, from the decomposition of the modal fields (TE and TM modes), are used to determine the dispersion matrix and thus the characterization of a discontinuity in waveguide. We extended the application of MM technique to the anisotropic material. By using modal analysis, our approach has considerably reduced the computation time compared to High Frequency Structure Simulator (HFSS) software.

Keywords: anisotropic metamaterials, forward and backward waves, MM, modal analysis, waveguides discontinuity

1. Introduction

Guided modes in circular waveguides consist of metamaterials [1–13] have been studied in the literature. Many studies of propagation modes in this waveguides with isotropic media [14–17] or double negative metamaterials [18, 19] have been presented in the literature. However, the rigorous study of the dispersion of anisotropic metamaterials in circular waveguides presents a lack in the literature. In this chapter, we present an extension of the rigorous analysis of the propagation of electromagnetic waves in magnetic transverse (TM) and electric transverse (TE) modes in the case of anisotropic circular waveguides, who take account of the spatial distribution of the permittivity and permeability of the medium. In this

structure, the propagation modes are exploited. The effects of anisotropic parameter on cutoff frequencies and dispersion characteristics are discussed. Below the cutoff frequency, the back backward waves can propagate in an anisotropic material. The numerical results with our MATLAB code for TM and TE modes were compared to theoretical predictions. Good agreements have been obtained. We analyzed a waveguide filters filled with partially anisotropic metamaterial using the mode matching (MM) technique based on the Scattering Matrix Approach (SMA) which, from the decomposition of the modal fields, are used to determine the dispersion matrix and thus the characterization of a discontinuity in waveguide. We extended the application of MM technique to the anisotropic material.

This formulation can be a useful tool for engineers of microwave. The metamaterial is largely applied by information technology industries, particularly in the radio frequency devices and microwaves such as the waveguide antennas, the patch antennas, the circulators, the resonators and the filters.

2. Formulation

In the anisotropic diagonal metamaterials medium, the Maxwell equations are expressed as follows

$$\vec{\nabla} \times \vec{E} = -j\omega\bar{\bar{\mu}}.\vec{H} \tag{1}$$

$$\vec{\nabla} \times \vec{H} = j\omega\bar{\bar{\varepsilon}}.\vec{E} \tag{2}$$

with

$$\bar{\bar{\mu}} = \mu_0 \begin{pmatrix} \mu_{rr} & 0 & 0 \\ 0 & \mu_{r\theta} & 0 \\ 0 & 0 & \mu_{rz} \end{pmatrix} = \mu_0 \begin{pmatrix} \mu_{rt} & 0 \\ 0 & \mu_{rz} \end{pmatrix}. \tag{3}$$

and

$$\bar{\bar{\varepsilon}} = \varepsilon_0 \begin{pmatrix} \varepsilon_{rr} & 0 & 0 \\ 0 & \varepsilon_{r\theta} & 0 \\ 0 & 0 & \varepsilon_{rz} \end{pmatrix} = \varepsilon_0 \begin{pmatrix} \varepsilon_{rt} & 0 \\ 0 & \varepsilon_{rz} \end{pmatrix} \tag{4}$$

Let consider a circular waveguide of radius R completely filled with anisotropic metamaterial without losses, as represented in the **Figure 1**. The wall of the guide is perfect conductor.

By considering the propagation in the Oz direction and manipulating Eqs. (1) and (2), we obtain the expressions of the transverse electromagnetic fields according to the longitudinal fields.

$$E_r = \frac{-j}{K_{c.r}^2}\left(k_z \frac{\partial E_z}{\partial r} + \frac{\omega\mu_0\mu_{r\theta}}{r}\frac{\partial H_z}{\partial \theta}\right) \tag{5}$$

$$E_\theta = \frac{j}{K_{c.\theta}^2}\left(\frac{-k_z}{r}\frac{\partial E_z}{\partial \theta} + \omega\mu_0\mu_{rr}\frac{\partial H_z}{\partial r}\right) \tag{6}$$

$$H_r = \frac{-j}{K_{c.\theta}^2}\left(-\frac{\omega\varepsilon_0\varepsilon_{r\theta}}{r}\frac{\partial E_z}{\partial \theta} + k_z \frac{\partial H_z}{\partial r}\right) \tag{7}$$

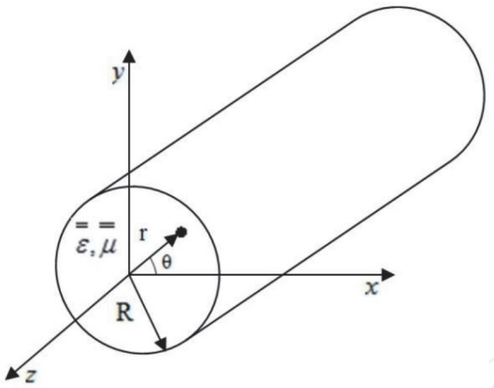

Figure 1.
Geometry of circular waveguide filled with metamaterial.

$$H_\theta = \frac{j}{K_{c.r}^2}\left(-\omega\varepsilon_0\varepsilon_{rr}\frac{\partial E_z}{\partial r} - \frac{k_z}{r}\frac{\partial H_z}{\partial \theta}\right) \tag{8}$$

with

$$K_{c.r}^2 = k_0^2\varepsilon_{rr}\mu_{r\theta} - k_z^2 \tag{9}$$

$$K_{c.\theta}^2 = k_0^2\varepsilon_{r\theta}\mu_{rr} - k_z^2 \tag{10}$$

$$k_0^2 = \omega^2\varepsilon_0\mu_0 \tag{11}$$

When E and H are the electric and magnetic field respectively. ε and μ are the permittivity and permeability. k_z is the propagation constant in z-direction.

In this chapter, we study rigorously the TE and TM modes in this anisotropic waveguide.

2.1 Transverse electric (TE) modes

From Eq. (1), the differential equation for z-component can be obtained as follows

$$\frac{\partial^2 H_z}{\partial r^2} + \frac{1}{r}\frac{\partial H_z}{\partial r} + \left(\frac{K_{c.\theta}^{(h)}\cdot\sqrt{\mu_{r\theta}}}{K_{c.r}^{(h)}\cdot\sqrt{\mu_{rr}}}\right)^2\frac{1}{r^2}\frac{\partial^2 H_z}{\partial \theta^2} + \left(\frac{\sqrt{\mu_{rz}}}{\sqrt{\mu_{rr}}}K_{c.\theta}^{(h)}\right)^2 H_z = 0. \tag{12}$$

Using the separation of the variables (r,θ), the expression of the longitudinal magnetic field H_z for the TE_{mn} modes in the circular metallic waveguide completely filled with anisotropic metamaterial is necessary for the resolution of the differential Eq. (12). H_z can be written as follows

$$H_z^{(h)} = H_0 \sin\left(\frac{K_{c.\theta}^{(h)}\cdot\sqrt{\mu_{r\theta}}}{K_{c.r}^{(h)}\cdot\sqrt{\mu_{rr}}}n.\theta\right)J_n\left(\frac{\sqrt{\mu_{rz}}}{\sqrt{\mu_{rr}}}K_{c.\theta}^{(h)}.r\right)e^{-jk_z z} \tag{13}$$

J_n is the Bessel function of the first kind of order n (n = 0, 1, 2, 3, ...).

The expressions (5)–(8) become

$$E_r^{(h)} = \frac{-j\omega\mu_0\mu_{r\theta}}{K_{c.r}^2.r}\left(\frac{K_{c.\theta}^{(h)}\cdot\sqrt{\mu_{r\theta}}}{K_{c.r}^{(h)}\cdot\sqrt{\mu_{rr}}}n.\theta\right)H_0.\cos\left(\frac{K_{c.\theta}^{(h)}\cdot\sqrt{\mu_{r\theta}}}{K_{c.r}^{(h)}\cdot\sqrt{\mu_{rr}}}n.\theta\right)J_n\left(\frac{\sqrt{\mu_{rz}}}{\sqrt{\mu_{rr}}}K_{c.\theta}^{(h)}.r\right)e^{-jk_z z} \tag{14}$$

$$E_\theta^{(h)} = \frac{j\omega\mu_0\mu_{rr}}{K_{c.\theta}^2}\left(\frac{\sqrt{\mu_{rz}}}{\sqrt{\mu_{rr}}}K_{c.\theta}^{(h)}\right)H_0.\sin\left(\frac{K_{c.\theta}^{(h)}\cdot\sqrt{\mu_{r\theta}}}{K_{c.r}^{(h)}\cdot\sqrt{\mu_{rr}}}n.\theta\right)J_n'\left(\frac{\sqrt{\mu_{rz}}}{\sqrt{\mu_{rr}}}K_{c.\theta}^{(h)}.r\right)e^{-jk_z z} \quad (15)$$

$$H_r^{(h)} = \frac{-jk_z}{K_{c.\theta}^2}\left(\frac{\sqrt{\mu_{rz}}}{\sqrt{\mu_{rr}}}K_{c.\theta}^{(h)}\right)H_0.\sin\left(\frac{K_{c.\theta}^{(h)}\cdot\sqrt{\mu_{r\theta}}}{K_{c.r}^{(h)}\cdot\sqrt{\mu_{rr}}}n.\theta\right)J_n'\left(\frac{\sqrt{\mu_{rz}}}{\sqrt{\mu_{rr}}}K_{c.\theta}^{(h)}.r\right)e^{-jk_z z} \quad (16)$$

$$H_\theta^{(h)} = \frac{-jk_z}{K_{c.r}^2.r}\left(\frac{K_{c.\theta}^{(h)}\cdot\sqrt{\mu_{r\theta}}}{K_{c.r}^{(h)}\cdot\sqrt{\mu_{rr}}}n\right)H_0.\cos\left(\frac{K_{c.\theta}^{(h)}\cdot\sqrt{\mu_{r\theta}}}{K_{c.r}^{(h)}\cdot\sqrt{\mu_{rr}}}n.\theta\right)J_n\left(\frac{\sqrt{\mu_{rz}}}{\sqrt{\mu_{rr}}}K_{c.\theta}^{(h)}.r\right)e^{-jk_z z} \quad (17)$$

With J_n' is the derivative of the Bessel function of the first kind of order n (n = 0, 1, 2, 3, ...).

The boundary conditions are written as follows:

$$E_\theta(r=R) = E_z(r=R) = 0 \quad (18)$$

Consequently, from Eq. (15), we obtain

$$J_n'\left(\frac{\sqrt{\mu_{rz}}}{\sqrt{\mu_{rr}}}K_{c.\theta}^{(h)}.R\right) = 0 \quad (19)$$

This implies

$$u_{nm}' = \frac{\sqrt{\mu_{rz}}}{\sqrt{\mu_{rr}}}K_{c.\theta}^{(h)}.R \quad (20)$$

Where u_{nm}' represents the mth zero (m = 1, 2, 3, ...) of the derivative of the Bessel function J_n' of the first kind of order n.

The constant H_0 is determined by normalizing the power flow down the circular guide.

$$P^{TE} = \int_0^R\int_0^{2\pi}\left(E_r^{(h)}H_\theta^{*(h)} - E_\theta^{(h)}H_r^{*(h)}\right)rdrd\theta = 1 \quad (21)$$

Where * indicates the complex conjugate.

Eq. (21) gives

$$H_0 = \frac{K_{c.r}^3}{\sqrt{\omega\mu_0 k_z}}\frac{\sqrt{\mu_{rz}}}{\mu_{r\theta}}N_{nm}^{(h)} \quad (22)$$

With

$$N_{nm}^{(h)} = \frac{1}{\sqrt{\frac{\sigma_n}{2}}.\left(\left(u_{nm}'\right)^2 - n^2\right)^{1/2}.J_n\left(u_{nm}'\right)} \quad (23)$$

$$\sigma_n = \begin{cases} 2\pi, & if\ n = 0 \\ \pi - \dfrac{\sin\left(4\pi a.\mathrm{n}\right)}{4\mathrm{a.n}}, & if\ n > 0 \end{cases} \quad (24)$$

$$a = \frac{K_{c.\theta}^{(h)}\cdot\sqrt{\mu_{r\theta}}}{K_{c.r}^{(h)}\cdot\sqrt{\mu_{rr}}} \quad (25)$$

Finally, the propagation constant in TE mode is given by

$$k_{z.nm}^{(TE)} = \pm\sqrt{k_0^2\varepsilon_{r\theta}.\mu_{rr} - \frac{\mu_{rr}}{\mu_{rz}}\left(\frac{u'_{nm}}{R}\right)^2} \tag{26}$$

The cutoff frequency is written

$$f_{c.nm}^{(TE)} = \frac{c}{2\pi}\frac{1}{\sqrt{|\varepsilon_{r\theta}\mu_{rz}|}}.\left(\frac{u'_{nm}}{R}\right). \tag{27}$$

We can introduce the following effective permeability and effective permittivity to describe the propagation characteristics of the waveguide modes [6, 7, 13].

$$\mu_{r,eff}^{TE} = \mu_{rr}, \tag{28}$$

$$\varepsilon_{r,eff}^{TE} = \varepsilon_{r\theta}\left(1 - \frac{1}{\varepsilon_{r\theta}\mu_{rz}k_0^2}.\left(\frac{u'_{nm}}{R}\right)^2\right). \tag{29}$$

Further, it is apparent that:

- $k_z^{TE} = k_0\sqrt{\mu_{r,eff}^{TE}.\varepsilon_{r,eff}^{TE}} > 0$, for $\mu_{r,eff}^{TE} > 0$ and $\varepsilon_{r,eff}^{TE} > 0$;
- $k_z^{TE} = -k_0\sqrt{\mu_{r,eff}^{TE}.\varepsilon_{r,eff}^{TE}} < 0$, for $\mu_{r,eff}^{TE} < 0$ and $\varepsilon_{r,eff}^{TE} < 0$;
- $k_z^{TE} = \pm jk_0\sqrt{\mu_{r,eff}^{TE}.\varepsilon_{r,eff}^{TE}}$, for $\mu_{r,eff}^{TE}.\varepsilon_{r,eff}^{TE} < 0$.

The sign of $\varepsilon_{r,eff}^{TE}$ depends on the sign of μ_{rz}. In the following, we will consider all cases that arise from the different sign of μ_{rz}.

2.1.1 First case $\mu_{rz} > 0$

For $\varepsilon_{r\theta} > 0$, we have.

$$\varepsilon_{r,eff}^{TE} = |\varepsilon_{r\theta}|\left(1 - \frac{1}{|\varepsilon_{r\theta}\,\mu_{rz}|k_0^2}.\left(\frac{u'_{nm}}{R}\right)^2\right) = |\varepsilon_{r\theta}|\left(1 - \left(\frac{f_{c.nm}^{TE}}{f}\right)^2\right) < 0, \text{ if } f < f_{c.nm}^{TE} \tag{30}$$

And for $\varepsilon_{r\theta} < 0$, $\varepsilon_{r,eff}^{TE}$ is rewritten as

$$\varepsilon_{r,eff}^{TE} = -|\,\varepsilon_{r\theta}|\left(1 + \frac{1}{|\,\varepsilon_{r\theta}\,\mu_{rz}|k_0^2}.\left(\frac{u'_{nm}}{R}\right)^2\right) < 0. \tag{31}$$

It can be seen that $\mu_{rz} > 0$ leads to $\varepsilon_{r,eff}^{TE} < 0$ below the cutoff frequency whenever $\varepsilon_{r\theta} > 0$ or $\varepsilon_{r\theta} < 0$.

2.1.2 Second case $\mu_{rz} < 0$

For $\varepsilon_{r\theta} > 0$, $\varepsilon_{r,eff}^{TE}$ is rewritten as

$$\varepsilon_{r,eff}^{TE} = |\varepsilon_{r\theta}|\left(1 + \frac{1}{|\varepsilon_{r\theta}\,\mu_{rz}|k_0^2}\cdot\left(\frac{u'_{nm}}{R}\right)^2\right) > 0. \tag{32}$$

And for $\varepsilon_{r\theta} < 0$, we obtain.

$$\begin{aligned}\varepsilon_{r,eff}^{TE} &= -|\varepsilon_{r\theta}|\left(1 - \frac{1}{|\varepsilon_{r\theta}\,\mu_{rz}|k_0^2}\cdot\left(\frac{u'_{nm}}{R}\right)^2\right)\\ &= -|\varepsilon_{r\theta}|\left(1 - \left(\frac{f_{c.nm}^{TE}}{f}\right)^2\right) > 0, \text{ if } f < f_{c.nm}^{TE}.\end{aligned} \tag{33}$$

Consequently, $\mu_{rz} < 0$ leads to $\varepsilon_{r,eff}^{TE} > 0$ below the cutoff frequency whenever $\varepsilon_{r\theta} > 0$ or $\varepsilon_{r\theta} < 0$.

Therefore, the relative permeability μ_{rz} below the cutoff frequency determines the sign of the relative effective permittivity of the anisotropic metamaterial in the circular waveguide. And the sign of the product $\mu_{rr}.\mu_{rz}$ of the metamaterial below the cutoff frequency determines the sign of the propagation constants of the waveguide studied.

The backward waves are obtained for $\mu_{rr} < 0$ and $\mu_{rz} > 0$ and the forward waves for $\mu_{rr} > 0$ and $\mu_{rz} < 0$ and. Therefore, the backward waves and the forward waves can propagate below the cutoff frequency.

2.2 Transverse magnetic (TM) modes

Similar to TE modes, TM modes can be derived as follows:
From Eq. (2), the differential equation for z-component can be obtained

$$\frac{\partial^2 E_z}{\partial r^2} + \frac{1}{r}\frac{\partial E_z}{\partial r} + \left(\frac{K_{c.r}^{(e)}\cdot\sqrt{\varepsilon_{r\theta}}}{K_{c.\theta}^{(e)}\cdot\sqrt{\varepsilon_{rr}}}\right)^2\frac{1}{r^2}\frac{\partial^2 E_z}{\partial\theta^2} + \left(\frac{\sqrt{\varepsilon_{rz}}}{\sqrt{\varepsilon_{rr}}}K_{c.r}^{(e)}\right)^2 E_z = 0. \tag{34}$$

Using the separation of the variables (r,θ), the expression of the longitudinal electric field E_z for the TM_{nm} modes in the circular metallic waveguide completely filled with anisotropic metamaterial is necessary for the resolution of the differential Eq. (34). E_z can be written as follows

$$E_z^{(e)} = E_0\cos\left(\frac{K_{c.\theta}^{(e)}\cdot\sqrt{\varepsilon_{rr}}}{K_{c.r}^{(e)}\cdot\sqrt{\varepsilon_{r\theta}}}n.\theta\right)J_n\left(\frac{\sqrt{\varepsilon_{rz}}}{\sqrt{\varepsilon_{rr}}}K_{c.r}^{(e)}.r\right)e^{-jk_z z} \tag{35}$$

The expressions (5)–(8) become

$$E_r^{(e)} = \frac{-jk_z}{K_{c.r}}\frac{\sqrt{\varepsilon_{rz}}}{\sqrt{\varepsilon_{rr}}}E_0.\cos\left(\frac{K_{c.\theta}^{(e)}\cdot\sqrt{\varepsilon_{rr}}}{K_{c.r}^{(e)}\cdot\sqrt{\varepsilon_{r\theta}}}n.\theta\right)J_n'\left(\frac{\sqrt{\varepsilon_{rz}}}{\sqrt{\varepsilon_{rr}}}K_{c.r}^{(e)}.r\right)e^{-jk_z z} \tag{36}$$

$$E_\theta^{(e)} = \frac{jk_z}{K_{c.\theta}.K_{c.r}}\frac{\sqrt{\varepsilon_{rr}}}{\sqrt{\varepsilon_{r\theta}}}\frac{n}{r}E_0.\sin\left(\frac{K_{c.\theta}^{(e)}\cdot\sqrt{\varepsilon_{rr}}}{K_{c.r}^{(e)}\cdot\sqrt{\varepsilon_{r\theta}}}n.\theta\right)J_n\left(\frac{\sqrt{\varepsilon_{rz}}}{\sqrt{\varepsilon_{rr}}}K_{c.r}^{(e)}.r\right)e^{-jk_z z} \tag{37}$$

$$H_r^{(e)} = \frac{-j\omega\varepsilon_0}{K_{c.\theta}.K_{c.r}}\sqrt{\varepsilon_{r\theta}}\sqrt{\varepsilon_{rr}}.\frac{n}{r}E_0.\sin\left(\frac{K_{c.\theta}^{(e)}.\sqrt{\varepsilon_{rr}}}{K_{c.r}^{(e)}.\sqrt{\varepsilon_{r\theta}}}n.\theta\right)J_n\left(\frac{\sqrt{\varepsilon_{rz}}}{\sqrt{\varepsilon_{rr}}}K_{c.r}^{(e)}.r\right)e^{-jk_z z} \tag{38}$$

$$H_\theta^{(e)} = \frac{-j\omega\varepsilon_0}{K_{c.r}}\sqrt{\varepsilon_{rr}}\sqrt{\varepsilon_{rz}}.E_0.\cos\left(\frac{K_{c.\theta}^{(e)}.\sqrt{\varepsilon_{rr}}}{K_{c.r}^{(e)}.\sqrt{\varepsilon_{r\theta}}}n.\theta\right)J_n'\left(\frac{\sqrt{\varepsilon_{rz}}}{\sqrt{\varepsilon_{rr}}}K_{c.r}^{(e)}.r\right)e^{-jk_z z} \tag{39}$$

The boundary condition (18) gives the following equation

$$J_n(u_{nm}) = 0. \tag{40}$$

with

$$u_{nm} = \frac{\sqrt{\varepsilon_{rz}}}{\sqrt{\varepsilon_{rr}}}K_{c.r}^{(e)}.R. \tag{41}$$

In Eq. (41) u_{nm} represents the mth zero (m = 1, 2, 3, ...) of the Bessel function J_n of the first kind of order n.

The constant E_0 is determined by normalizing the power flow down the circular guide.

$$P^{TM} = \int_0^R\int_0^{2\pi}\left(E_r^{(e)}H_\theta^{*(e)} - E_\theta^{(e)}H_r^{*(e)}\right)rdrd\theta = 1 \tag{42}$$

Eq. (42) gives:

$$E_0 = \frac{K_{c.r}^2}{\sqrt{\omega\varepsilon_0\varepsilon_{rr}}k_z}N_{nm}^{(e)} \tag{43}$$

with

$$N_{nm}^{(e)} = \frac{1}{u_{nm}.J_n'(u_{nm}).\sqrt{\frac{\delta_n}{2}}} \tag{44}$$

$$\delta_n = \begin{cases} 2\pi, \ if\ n = 0 \\ \pi - \dfrac{\sin(4\pi b.\mathrm{n})}{4\mathrm{b.n}}, \ if\ n > 0 \end{cases} \tag{45}$$

$$b = \frac{K_{c.\theta}^{(e)}.\sqrt{\varepsilon_{rr}}}{K_{c.r}^{(e)}.\sqrt{\varepsilon_{r\theta}}} \tag{46}$$

Finally, the propagation constant in TM mode is given by:

$$k_{z.nm}^{(TM)} = \pm\sqrt{k_0^2\varepsilon_{rr}.\mu_{r\theta} - \frac{\varepsilon_{rr}}{\varepsilon_{rz}}\left(\frac{u_{nm}}{R}\right)^2} \tag{47}$$

Obviously, the cutoff frequency is written

$$f_{c.nm}^{(TM)} = \frac{c}{2\pi}\frac{1}{\sqrt{|\mu_{r\theta}\varepsilon_{rz}|}}.\left(\frac{u_{nm}}{R}\right). \tag{48}$$

We can introduce the following effective permeability and effective permittivity to describe the propagation characteristics of the waveguide modes.

$$\varepsilon_{r,eff}^{TM} = \varepsilon_{rr}, \tag{49}$$

$$\mu_{r,eff}^{TM} = \mu_{r\theta}\left(1 - \frac{1}{\mu_{r\theta}\varepsilon_{rz}k_0^2}.\left(\frac{u_{nm}}{R}\right)^2\right). \tag{50}$$

Similar to the previous discussion, we have three possibilities:
Further, It is apparent that:

- $k_z^{TM} = k_0\sqrt{\mu_{r,eff}^{TM}.\varepsilon_{r,eff}^{TM}} > 0$, for $\mu_{r,eff}^{TM} > 0$ and $\varepsilon_{r,eff}^{TM} > 0$;
- $k_z^{TM} = -k_0\sqrt{\mu_{r,eff}^{TM}.\varepsilon_{r,eff}^{TM}} < 0$, for $\mu_{r,eff}^{TM} < 0$ and $\varepsilon_{r,eff}^{TM} < 0$;
- $k_z^{TM} = \pm jk_0\sqrt{\mu_{r,eff}^{TM}.\varepsilon_{r,eff}^{TM}}$, for $\mu_{r,eff}^{TM}.\varepsilon_{r,eff}^{TM} < 0$.

Consequently, the sign of $\mu_{r,eff}^{TM}$ depends on the sign of ε_{rz}. In the following, we will consider all cases that arise from the different sign of ε_{rz}.

2.2.1 Case when $\varepsilon_{rz} > 0$

In this case, for $\mu_{r\theta} > 0$, $\mu_{r,eff}^{TM}$ is rewritten as.

$$\mu_{r,eff}^{TM} = |\mu_{r\theta}|\left(1 - \frac{1}{|\mu_{r\theta}\,\varepsilon_{rz}|k_0^2}.\left(\frac{u_{nm}}{R}\right)^2\right) = |\mu_{r\theta}|\left(1 - \left(\frac{f_{c.nm}^{TM}}{f}\right)^2\right) < 0, \text{ if } f < f_{c.nm}^{TM} \tag{51}$$

And for $\mu_{r\theta} < 0$, we have

$$\mu_{r,eff}^{TM} = -|\mu_{r\theta}|\left(1 + \frac{1}{|\mu_{r\theta}\varepsilon_{rz}|k_0^2}.\left(\frac{u_{nm}}{R}\right)^2\right) < 0. \tag{52}$$

It can be seen that $\varepsilon_{rz} > 0$ leads to $\mu_{r,eff}^{TM} < 0$ below the cutoff frequency whenever $\mu_{r\theta} > 0$, or $\mu_{r\theta} < 0$.

2.2.2 Case when $\varepsilon_{rz} < 0$

In this case, for $\mu_{r\theta} > 0$, we have

$$\mu_{r,eff}^{TM} = |\mu_{r\theta}|\left(1 + \frac{1}{|\mu_{r\theta}\,\varepsilon_{rz}|k_0^2}.\left(\frac{u_{nm}}{R}\right)^2\right) > 0. \tag{53}$$

and for $\mu_{r\theta} < 0$, we obtain.

$$\mu_{r,eff}^{TM} = -|\mu_{r\theta}|\left(1 - \frac{1}{|\mu_{r\theta}\,\varepsilon_{rz}|k_0^2}.\left(\frac{u_{nm}}{R}\right)^2\right) = -|\mu_{r\theta}|\left(1 - \left(\frac{f_{c.nm}^{TM}}{f}\right)^2\right) > 0., \text{ if } f < f_{c.nm}^{TM} \tag{54}$$

It is also seen that the relative permittivity ε_{rz} which is independent of $\mu_{r\theta}$ determines the sign of the relative effective permeability $\mu_{r,eff}^{TM}$ of the anisotropic metamaterial in the circular waveguide. The forward wave propagates in the waveguide for $\varepsilon_{rz} < 0$ and $\varepsilon_{rr} > 0$, and backward wave propagates for $\varepsilon_{rz} > 0$ and $\varepsilon_{rr} < 0$.

Therefore from this analysis, it is found that both the backward waves and the forward waves can propagate in any frequency region. This is determined by the sign of ε_{rz} and ε_{rr} for TM modes and the sign of μ_{rz} and μ_{rr} for TE modes.

2.3 Analysis of uniaxial discontinuities in the circular waveguides

In this section, we analyzed a waveguide filters filled with partially anisotropic metamaterial using the extension of the mode matching technique based on the Scattering Matrix Approach which, from the decomposition of the modal fields, are used to determine the dispersion matrix and thus the characterization of a discontinuity in waveguide. The discontinuities are considered without losses.

In **Figure 2** we consider a junction between two circular waveguides having the same cross section filled with two different media. a^i and b^i are the incident and the reflected waves, respectively.

The transverse electric and magnetic fields (E_T, H_T) in the wave guides can be written in the modal bases as follows [20]:

$$E_T = \sum_{m=1}^{\infty} A_m^i \left(a_m^i + b_m^i\right) e_m^i \tag{55}$$

$$H_T = \sum_{m=1}^{\infty} B_m^i \left(a_m^i - b_m^i\right) h_m^i \tag{56}$$

where H_T and E_T are the transverse magnetic and electric fields (T refers to the components in the transverse plane), h_m^i, e_m^i represent the mth magnetic and electric modal Eigen function in the guide i, respectively and A_m^i and B_m^i are complex coefficients which are determined by normalizing the power flow down the circular guides (m is the index of the mode and i = *I, II*).

At the junction, the continuity of the fields allows to write the following equations:

$$E_t^I = E_t^{II} \tag{57}$$

$$H_t^I = H_t^{II} \tag{58}$$

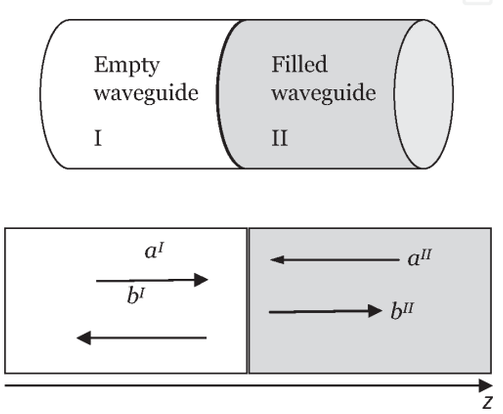

Figure 2.
Junction between two circular waveguides filled with two different media having the same cross section.

By postponing the Eqs. (55) and (56) in (57) and (58), we obtain:

$$\sum_{m=1}^{N_1} A_m^I \left(a_m^I + b_m^I\right) e_m^I = \sum_{p=1}^{N_2} A_p^{II} \left(a_p^{II} + b_p^{II}\right) e_p^{II} \tag{59}$$

$$\sum_{m=1}^{N_1} B_m^I \left(a_m^I - b_m^I\right) h_m^I = \sum_{p=1}^{N_2} B_p^{II} \left(-a_p^{II} + b_p^{II}\right) h_p^{II} \tag{60}$$

N_1 and N_2 are the number of considered modes in guides 1 and 2, respectively. By applying the Galerkin method, Eqs. (59) and (60), lead to the following systems:

$$\sum_{m=1}^{N_1} A_m^I \left(a_m^I + b_m^I\right) \left\langle e_m^I | e_p^{II} \right\rangle = A_p^{II} \left(a_p^{II} + b_p^{II}\right) \tag{61}$$

$$B_m^I \left(a_m^I - b_m^I\right) = \sum_{p=1}^{N_2} B_p^{II} \left(-a_p^{II} + b_p^{II}\right) \left\langle h_p^{II} | h_m^I \right\rangle \tag{62}$$

The inner product is defined as:

$$\langle e_m | e_p \rangle = \int_S e_m^* e_p \, dS \tag{63}$$

The Eqs. (61) and (62) give:

$$-a_p^{II} + \sum_{m=1}^{N_1} \frac{A_m^I}{A_p^{II}} a_m^I \left\langle e_m^I | e_p^{II} \right\rangle = b_p^{II} - \sum_{m=1}^{N_1} \frac{A_m^I}{A_p^{II}} b_m^I \left\langle e_m^I | e_p^{II} \right\rangle \tag{64}$$

$$a_m^I + \sum_{p=1}^{N_2} \frac{B_p^{II}}{B_m^I} a_p^{II} \left\langle h_p^{II} | h_m^I \right\rangle = b_m^I + \sum_{p=1}^{N_2} \frac{B_p^{II}}{B_m^I} b_p^{II} \left\langle h_p^{II} | h_m^I \right\rangle \tag{65}$$

which can be written in matrix form:

$$\begin{bmatrix} U & M_1 \\ M_2 & -U \end{bmatrix} \begin{bmatrix} a_1^I \\ . \\ a_{N_1}^I \\ a_1^{II} \\ . \\ a_{N_2}^{II} \end{bmatrix} = \begin{bmatrix} U & M_1 \\ -M_2 & U \end{bmatrix} \begin{bmatrix} b_1^I \\ . \\ b_{N_1}^I \\ b_1^{II} \\ . \\ b_{N_2}^{II} \end{bmatrix} \tag{66}$$

where U is the identity matrix. M_1 and M_2 are defined as:

$$M_{1ij} = \frac{B_j^{II}}{B_i^I} \left\langle h_j^{II} | h_i^I \right\rangle \tag{67}$$

$$M_{2ij} = \frac{A_i^I}{A_j^{II}} \left\langle e_i^I | e_j^{II} \right\rangle \tag{68}$$

The scattering matrix of the discontinuity is:

$$S = \begin{bmatrix} U & M_1 \\ -M_2 & U \end{bmatrix}^{-1} \begin{bmatrix} U & M_1 \\ M_2 & -U \end{bmatrix} \tag{69}$$

The total scattering matrix is obtained by chaining the S scattering matrices of all the discontinuities in a waveguide having cascaded uniaxial discontinuities [21].

3. Numerical results and discussion

3.1 Propagating modes

We choose the radius of the circular metal guide R = 13.4 mm.

In a first case, we study the TE modes of a circular guide completely filled with anisotropic metamaterials (see **Figure 1**) with negative μ_{rr} or negative μ_{rz}. The fundamental mode of the equivalent empty circular waveguide has a resonant frequency of 6.57 GHz. For the case of metamaterials with a permeability $\mu_r = -1$ and permittivity $\varepsilon_r = -4.4$, the fundamental mode presents a resonance frequency of $f_{c.11}^{TE} = 3.13\ GHz$.

In **Figure 3** the curves of the propagation constant, for frequency range 1–10 GHz and for the first five TE modes with $\mu_{rr} = 1$, $\mu_{rz} = -1$ and $\varepsilon_{r\theta} = 4.4$, are represented. We observe that all modes propagate without cutoff frequencies (forward waves). **Figure 4** represents the same diagrams for $\mu_{rr} = -1$, $\mu_{rz} = 1$ and $\varepsilon_{r\theta} = 4.4$. When n and m are small and ω is large, the waves stop propagating. So, these modes propagate at low frequencies and cutoff at high frequencies (backward waves).

It is interesting to see that both forward and backward waves can be obtained by controlling the signs of μ_{rz} and μ_{rr}. Our results agree well with the predicted ones.

In a second case, we study the TE modes of this circular waveguide. **Figure 5** represents the curves of propagation constant for the frequency range 1–10 GHz

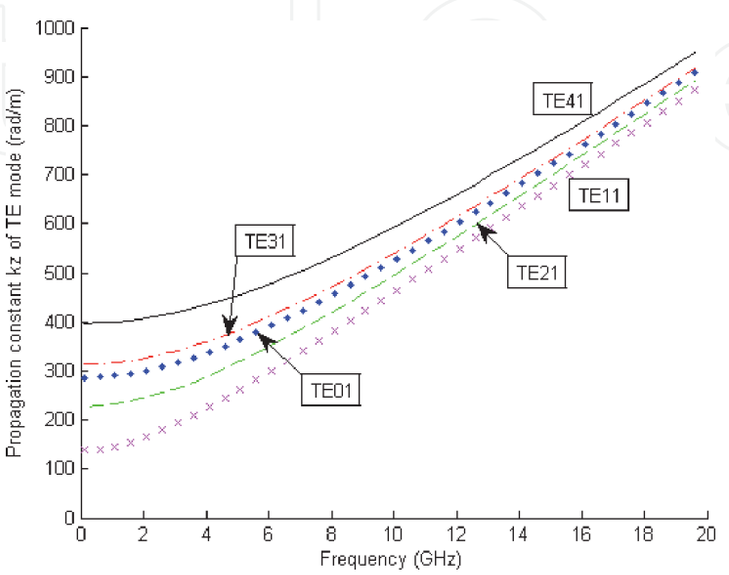

Figure 3.
Curves of propagation constant k_z^{TE} *for TE mode of the circular waveguide completely filled anisotropic metamaterial with parameters* $\mu_{rr} = 1$, $\mu_{rz} = -1$, $\varepsilon_{r\theta} = 4.4$.

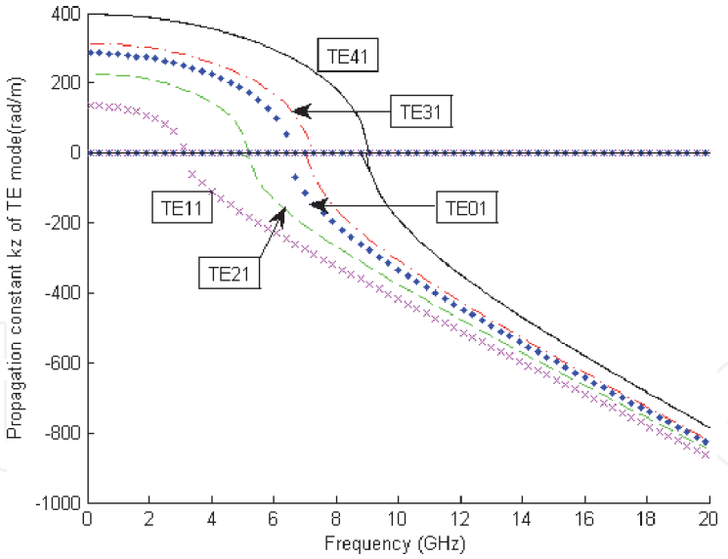

Figure 4.
Curves of propagation constant k_z^{TE} *for TE mode of the circular waveguide completely filled anisotropic metamaterial with parameters* $\mu_{rr} = -1$, $\mu_{rz} = 1$ *and* $\varepsilon_{r\theta} = 4.4$.

and for the first five TM modes with $\varepsilon_{rr} = 4.4$, $\varepsilon_{rz} = -4.4$ and $\mu_{r\theta} = 1$. All modes propagate without cutoff (forward waves).

Calculated curves of propagation constant for the frequency range 1–10 GHz and for the first five TM modes with $\varepsilon_{rr} = -4.4$, $\varepsilon_{rz} = 4.4$, $\mu_{r\theta} = 1$ are presented. We notice that both forward wave and backward wave can be obtained by controlling the signs of ε_{rr} and ε_{rz}. **Figures 5** and **6** show that our results agree well with the predicted ones.

We observe that the cutoff frequencies of lowest TE modes decreased with the respect increase of μ_{rz} for $\mu_{rr} = -1$ and $\varepsilon_{r\theta} = 4.4$ (see **Figure 7**). In a same manner, the TM cutoff frequencies decreased with the respect increase of ε_{rz} for $\varepsilon_{rr} = -4.4$ and $\mu_{r\theta} = 1$ (see **Figure 8**). Consequently, by varying the parameters of material the propagating mode can be controlled.

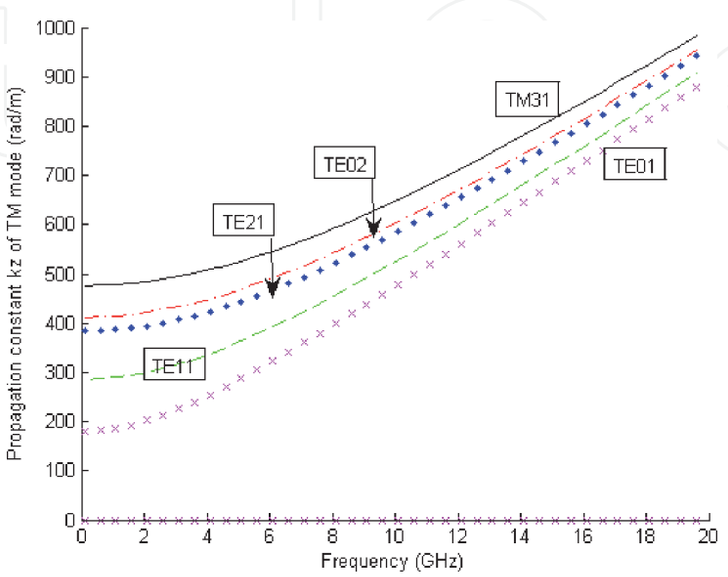

Figure 5.
Curves of propagation constant k_z^{TM} *for TM mode of the circular waveguide completely filled anisotropic metamaterial with parameters* $\varepsilon_{rr} = 4.4$, $\varepsilon_{rz} = -4.4$, $\mu_{r\theta} = 1$.

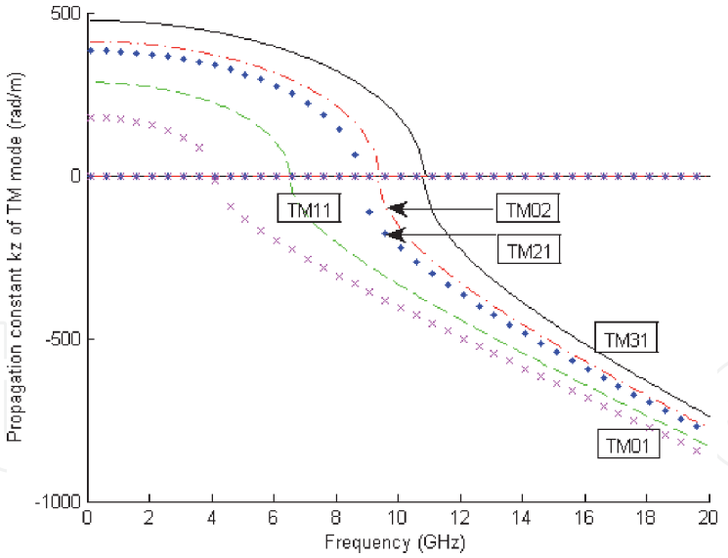

Figure 6.
Curves of propagation constant k_z^{TM} for TM mode of the circular waveguide completely filled anisotropic metamaterial with parameters $\varepsilon_{rr} = -4.4$, $\varepsilon_{rz} = 4.4$, $\mu_{r\theta} = 1$.

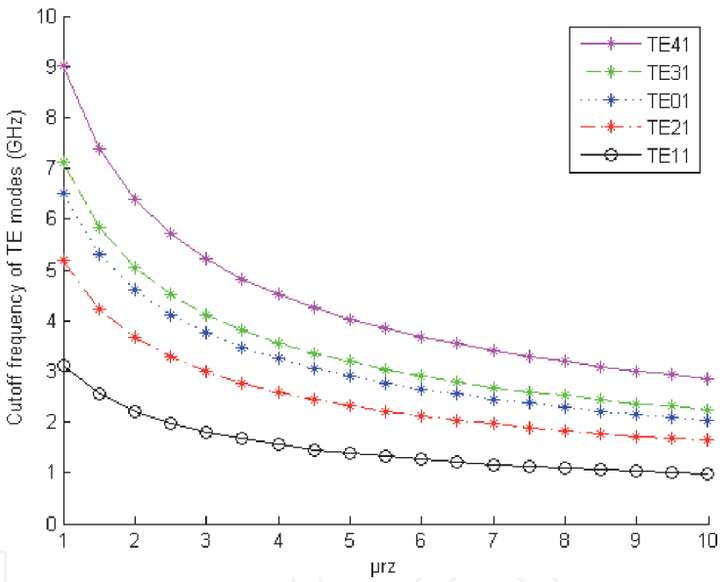

Figure 7.
The cutoff frequencies for the first five TE modes versus μ_{rz} with $\mu_{rr} = -1$, $\varepsilon_{r\theta} = 4.4$.

3.2 Filter design

We consider now, 12 discontinuities (see **Figure 9**) constituted by juxtaposing 13 circular waveguides having the same dimensions (R = 13.4 mm). The circuit is formed by alternation of empty guide ($\varepsilon_r = \mu_r = 1$) of width l = 10 mm and guide filled by anisotropic metamaterials ($\varepsilon_{rr} = \varepsilon_{r\theta} = -\varepsilon_{rz} = -4.4$; $\mu_{rr} = \mu_{r\theta} = -\mu_{rz} = 1$) of width d = 0.2 mm (periodic structure). **Figure 9** represents the geometry of the studied structure.

The transmission and reflection coefficients using our numerical method with MATLAB and HFSS are presented in **Figure 10**. We used 8 modes in the whole circuit for the modal method. The simulations results show that are in perfect agreement. However and especially if the number of discontinuities increases, our method is significantly faster than HFSS. Then, by using our approach, it could easy to design filters according to a given specifications.

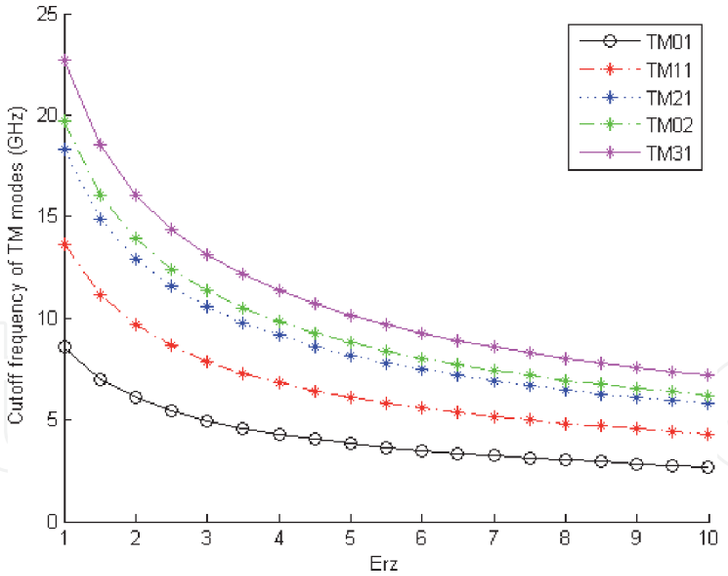

Figure 8.
The cutoff frequencies for the first five TM modes versus ε_{rz} with $\varepsilon_{rr} = -4.4$, $\mu_{r\theta} = 1$.

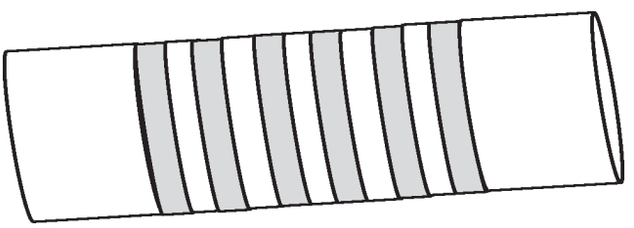

Figure 9.
Geometry of the circular waveguide with 12 discontinuities.

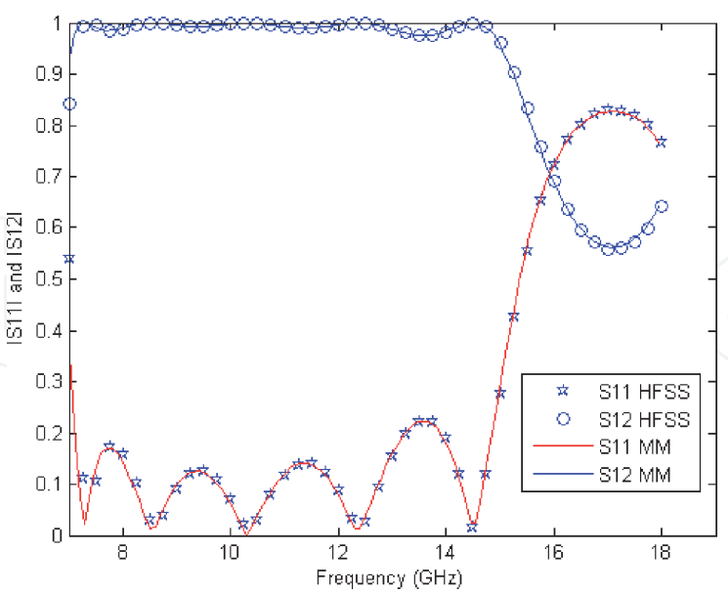

Figure 10.
Reflection coefficient of the periodic structure with 12 discontinuities.

4. Conclusion

Rigorous analysis of propagating modes in circular waveguides filled with anisotropic metamaterial has been developed. It was demonstrated that the

propagation constant of the waveguide are closely dependent on constitutive parameters of the metamaterial. Using our MATLAB code the dispersion curves of the fundamental mode and the first four higher order modes of the metamaterial waveguide are obtained.

We found that in different frequency ranges below and above the cutoff frequency both the forward and the backward waves can propagate. This is determined by the sign of ε_{rz} and ε_{rr} for TM modes and by the sign of μ_{rz} and μ_{rr} for TE modes. Our simulation results are in good agreement with the theoretical prediction.

Moreover, using the Scattering Matrix Approach we applied the extension of MM technique to determine the dispersion matrix and to analyze multiple uniaxial circular discontinuity in waveguide filled with anisotropic metamaterials. This introduced tool is applied to the modeling of large complex structures such as filters where its rapidity compared to the commercial simulation tools is verified.

Author details

Hedi Sakli[1,2*] and Wyssem Fathallah[1]

1 MACS Research Laboratory, National Engineering School of Gabes, Gabes University, Gabes, Tunisia

2 EITA Consulting, Montesson France

*Address all correspondence to: hedi.s@eitaconsulting.fr

IntechOpen

References

[1] Alu A, Engheta N. Mode excitation by a line source in a parallel plate waveguide filled with a pair of parallel double-negative and double-positive slabs. In: IEEE AP-S International Symposium. Columbus, OH; 2003. pp. 359-362

[2] Xu Y. Wave propagation in rectangular waveguide filled with single negative metamaterial slab. Electronics Letters. 2003;**39**(25):1831-1833

[3] Xu Y. A study of waveguides field with anisotropic metamaterials. Microwave and Optical Technology Letters. 2004;**41**:426-431

[4] Alu A, Engheta N. Guided modes in a waveguide filled with a pair of single-negative (SNG), double negative (DNG), and/or double-positive (DPS) layers. IEEE Transactions on Microwave Theory and Techniques. 2004;**52**: 199-210

[5] Cory H, Shtrom A. Wave propagation along a rectangular metallic waveguide longitudinally loaded with a metamaterial slab. Microwave and Optical Technology Letters. 2004;**41**(2): 123-127

[6] Meng FY, Wu Q, Fu JH, Gu XM, Li LW. Transmission characteristics of wave modes in a rectangular waveguide filled with anisotropic metamaterial. Applied Physics A: Materials Science & Processing. 2009;**94**:747-753

[7] Meng FY, Wu Q, Li LW. Controllable Metamaterial-loaded waveguides supporting backward and forward waves transmission characteristics of wave modes in a rectangular waveguide filled with anisotropic metamaterial. IEEE Transactions on Antennas and Propagation. 2011;**59**(9):3400-3411

[8] Zhang D, Ma J. The propagation and cutoff frequencies of the rectangular metallic waveguide partially filled with metamaterial multilayer slabs. Progress In Electromagnetics Research (PIER) M. 2009;**9**:35-40

[9] Pan Y, Xu S. Cpmlex modes in parallel-plate waveguide structure filled with left-handed material. Chinese Journal of Electronics. 2009;**18**(3): 551-554

[10] Cojocaru E. Waveguides filled with bilayers of double-negative (DNG) and double-positive (DPS) metamaterials. Progress In Electromagnetics Research (PIER) B. 2011;**32**:75-90

[11] Fathallah W, Sakli H, Aguili T. Electromagnetic wave propagation in anisotropic Metamaterial waveguides. International Journal of Numerical Modelling: Electronic Networks, Devices and Fields. 2015;**28**(4):479-486

[12] Fathallah W, Sakli H, Aguili T. Full-wave study of rectangular metamaterial waveguides using Galerkin's method. In: 8th International Multi-Conference on Systems, Signals and Devices, SSD'13, March 2013. Hammamet, Tunisia;

[13] Marques R, Martel J, Mesa F, Medina F. Left-handed-media simulation and transmission of EM waves in subwavelength split-ring-resonator-loaded metallic waveguides. Physical Review Letters. 2002;**89**:183901

[14] Balanis CA. Circular waveguides. In: Material in Advanced Engineering Electromagnetics. Vol. 9. New York: Wiley; 1989. pp. 643-650

[15] Boyenga DL, Mabika CN, Diezaba A. A new multimodal Variational formulation analysis of cylindrical waveguide uniaxial discontinuities. Research Journal of Applied Sciences, Engineering and Technology. 2013;**6**(5):787-792

[16] Thabet R, Riabi ML, Belmeguenai M. Rigorous design and efficient optimization of quarter-wave transformers in metallic circular waveguides using the mode-matching method and the genetic algorithm. Progress in Electromagnetics Research. 2007;**68**:15-33

[17] Mahmoud SF. Guided modes on open chirowaveguides. IEEE Transactions on Microwave Theory and Techniques. 1995;**43**(1):205-209

[18] Shadrivov IV, Sukhorukov AA, Kivshar YS. Guided modes in negative-refractive-index waveguides. Physical Review E. 2003;**67**:057602

[19] Dong J-F, Li J. Characteristics of guided modes in uniaxial chiral circular waveguides. Progress in Electromagnetics Research. 2012;**124**: 331-345

[20] Couffignal P. Contribution à l'étude Des Filters en Guides métalliques [thesis]. INP Toulouse; 1992

[21] Ghosh B, Kakade AB. Guided modes in a metamaterial-filled circular waveguide. Electromagnetics. 2012;**32**: 465-480